

## Butt-joint integrated InAs/InP quantum dot Fabry-Pérot laser devices emitting at 1.5 $\mu\text{m}$

H. Wang, J. Yuan, S. Ananthanasarn, P.J. van Veldhoven, T. de Vries, E. Smalbrugge, E.J. Geluk, E.A.J.M. Bente, Y.S. Oei, M.K. Smit, and R. Nötzel

COBRA Research Institute, Eindhoven University of Technology, 5600 MB Eindhoven, The Netherlands  
h.wang@tue.nl

**Abstract.** *Butt-joint integrated extended cavity InAs/InP (100) quantum dot (QD) Fabry-Pérot laser devices emitting around 1.55  $\mu\text{m}$  are demonstrated. Continuous wave lasing at room temperature is realized with devices of different lengths. The threshold currents, transparency current density, and external differential quantum efficiency are all comparable to those of all-active QD lasers. The Butt-joint reflectivity for straight waveguides is below -40 dB. Light versus current curves and lasing spectra reveal that for low current, lasing starts on the QD ground state transition, while excited state lasing sets in with increasing current.*

Monolithically integrated quantum dot (QD) laser devices for photonic integrated circuits have been realized in the InAs/GaAs materials system by selective area – and regrowth techniques [1,2]. We demonstrate the first Butt-joint active-passive integrated QD laser device in the InAs/InP (100) materials system emitting in the technologically important 1.55  $\mu\text{m}$  wavelength region for fiber based optical telecommunication systems. The extended cavity Fabry-Pérot QD laser operates in continuous wave (CW) mode at room temperature (RT) on the QD ground state (GS) transition. The threshold current, transparency current density, and external differential quantum efficiency are comparable to those of our all-active Fabry-Pérot QD lasers [3]. The Butt-joint reflectivity is below -40 dB for straight waveguides. Double-state lasing on the QD GS and excited state (ES) is observed with increasing injection current, which is caused by the inter-level relaxation rate of carriers typical for QDs [4].

**Device fabrication:** The integrated QD laser structure was grown by Metal-Organic Vapor Phase epitaxy (MOVPE) in a three-step process [5]. In the first epitaxy step, the active layer was grown on n-doped InP (100) substrate. It consists of a stack of five QD layers embedded in the center of a 500 nm thick  $\lambda = 1250$  nm lattice-matched InGaAsP (Q1.25) layer. The average QD diameter, height, and density are 50 nm, 5.6 nm, and  $2 \times 10^{10} \text{ cm}^{-2}$ , and the Q1.25 separation layers are 40 nm thick. The emission wavelength of the 3-monolayers (MLs) InAs QDs was tuned into the 1.55  $\mu\text{m}$  wavelength region through insertion of ultrathin (1.3 MLs) GaAs interlayers underneath the QDs [6]. Then a p-doped 200 nm thick InP layer was grown. Active mesa blocks were defined by photolithography using a 100 nm  $\text{SiN}_x$  layer as etching mask. The mesa blocks are 30  $\mu\text{m}$  wide and spaced apart by 250  $\mu\text{m}$  with lengths varying from 200 to 2000  $\mu\text{m}$ . The future passive areas were etched wet chemically 50 nm below the active layer, thus 560 nm were etched for regrowth. An overhang below the  $\text{SiN}_x$  mask prevents the lateral overgrowth at the Butt-joint. Then undoped Q1.25 and InP layers were regrown by selective area MOVPE using the same  $\text{SiN}_x$  mask. The thicknesses of both layers are matched to the original thicknesses. The  $\text{SiN}_x$  mask was removed and the 1.5  $\mu\text{m}$  gradually p-doped InP top cladding and compositionally graded p-doped InGaAsP

contact layer were grown. After growth, straight ridge waveguides with a width of  $2\ \mu\text{m}$  were fabricated by reactive-ion dry etching  $100\ \text{nm}$  into the Q1.25 layer. The structure was planarized by polyimide and Ti/Pt/Au contact layers were fabricated on the active region and the back side. The extended cavity laser structures under investigation have a total length of  $2250\ \mu\text{m}$ . The active waveguide with length of  $1450$ ,  $1200$  and  $750\ \mu\text{m}$  in different devices is connected to one passive waveguide with length of  $800$ ,  $1050$  and  $1550\ \mu\text{m}$ , respectively. The integrated laser structures are terminated by cleaved mirrors on both ends, as shown in Fig 1.

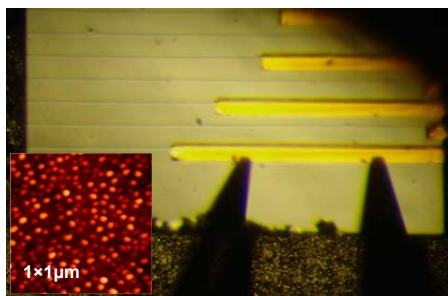


Fig. 1: Photograph of the integrated extended cavity InAs/InP (100) quantum dot (QD) laser devices. The two current probes contact the laser with  $1450\ \mu\text{m}$  long active and  $800\ \mu\text{m}$  long passive waveguides. Inset: atomic force microscopy (AFM) image of uncapped QDs.

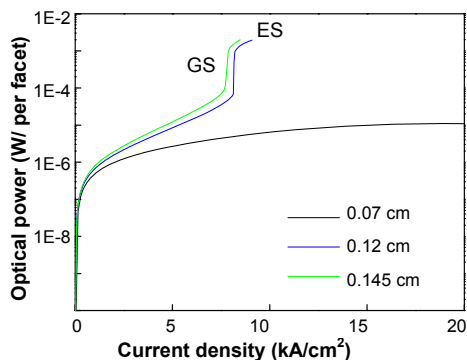


Fig. 2 light versus current (LI) curves of the integrated QD laser devices with different length of the active waveguides taken in continuous wave (CW) mode at room temperature (RT). The regimes of QD ground state (GS) and excited state (ES) lasing are indicated.

Results: Figure 2 shows the light versus current (LI) curves of the integrated laser structures with different length of the active waveguides. For the  $1450$  and  $1200\ \mu\text{m}$  long active waveguides, lasing occurs in CW mode at RT. The respective threshold currents are  $0.198\ \text{A}$  ( $6.76\ \text{kA}/\text{cm}^2$ ) and  $0.195\ \text{A}$  ( $8.13\ \text{kA}/\text{cm}^2$ ) and the external differential quantum efficiencies are  $7.26$  and  $2.75$ , similar to those of our all-active Fabry-Pérot QD lasers [3]. This confirms a low Butt-joint loss, which has been previously evaluated to be  $0.1 - 0.2\ \text{dB}$  in passive-passive structures [5]. From the length dependence of the threshold current, a transparency current density of  $116\ \text{A}/\text{cm}^2$ , i.e.,  $23.2\ \text{A}/\text{cm}^2$  per QD layer is estimated. The device with  $700\ \mu\text{m}$  long active waveguide does not show laser operation.

Lasing starts on the QD GS transition at  $1.53\ \mu\text{m}$  while ES lasing at shorter wavelength ( $1.50\ \mu\text{m}$ ) sets in with increasing current due to QD GS saturation. This leads to the characteristic step-like output power increase in the LI curves and is confirmed by the lasing spectra of the device with  $1200\ \mu\text{m}$  long active waveguide shown in Fig 3. When the current is increased from  $0.192\ \text{A}$  to  $0.194\ \text{A}$ , the GS emission intensity increases strongly while the ES emission intensity almost keeps constant. For further increase of the current from  $0.20\ \text{A}$  to  $0.220\ \text{A}$ , the GS emission intensity saturates, whereas the ES emission intensity steeply increases. Such double-state lasing phenomena are often

observed for self-assembled QD lasers, and caused by the carrier inter-level relaxation and recombination processes typical for QDs [4].

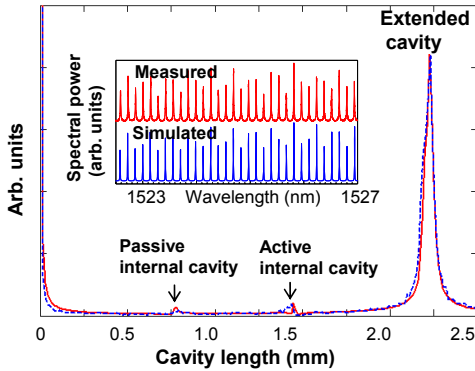


Fig. 3: Fourier Transforms of the experimental and fitted sub-threshold emission spectra. Inset: high resolution emission spectra. The active waveguide is 1450  $\mu\text{m}$ .

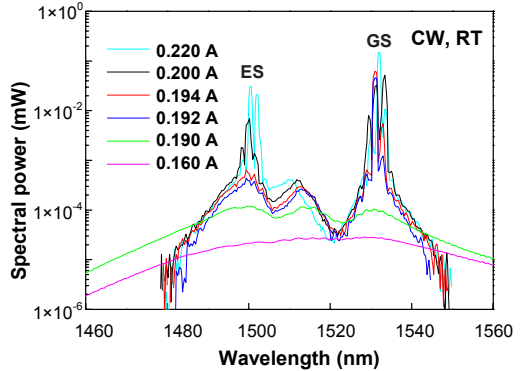


Fig. 4: Lasing spectra of the integrated QD laser with 1200  $\mu\text{m}$  long active waveguide for various currents (0.160 A, 0.190 A, 0.192 A, 0.194 A, 0.200 and 0.220 A). QD GS and ES transitions are indicated.

In addition to low Butt-joint absorption, a low Butt-joint reflectivity is essential for stable operation of photonic integrated devices and circuits. The Butt-joint reflectivity is measured based on the analysis of sub-threshold emission spectra which are recorded by an Optical Spectrum Analyzer (APEX AP2040) with a very high resolution of 0.16 pm [5]. By fitting the calculated sub-threshold mode structure to the recorded data, values of the reflectivity are extracted. Figure 4 depicts the Fourier Transforms of the experimental and fitted emission spectra, which are shown in the inset. In addition to the dominant peak in the Fourier Transform due to the extended cavity, small peaks are visible originating from the passive and active internal cavities formed by the cleaved mirrors and the Butt-joint. The extracted Butt-joint reflectivity is  $-42$  dB ( $6 \times 10^{-5}$ ). This is similar to the reflectivity of our Butt-joints examined with bulk active region extended cavity lasers and can easily be reduced to below  $-50$  dB using waveguides entering the Butt-joint under an angle [7].

**Conclusion:** We have demonstrated Butt-joint active-passive integrated extended cavity Fabry-Pérot laser devices based on InAs/InP (100) quantum dots (QDs) emitting around 1.55  $\mu\text{m}$ . Continuous wave lasing at room temperature on the QD ground state transition was achieved. The threshold current was comparable to all-active Fabry-Pérot QD lasers. With increasing current, double-state lasing occurs which is typical for QDs due to the specific carrier inter-level relaxation and recombination processes. A Butt-joint reflectivity  $< -40$  dB for straight waveguides was determined. Hence, compatibility of our InAs/InP (100) QD gain material with Butt-joint active-passive integration is demonstrated paving the way for QD based photonic integrated devices

and circuits operating in the technologically important 1.55  $\mu\text{m}$  wavelength region for fiber based optical telecommunication systems.

## References

- [1] S. Mokkalapati, H.H. Tan and C. Jagadish, 'Integration of an InGaAs quantum-dot laser with a low-loss passive waveguide using selective-area epitaxy', *IEEE Photon. Technol. Lett.*, vol. 18, pp. 1648-1650, 2006.
- [2] J. Yang, P. Bhattacharya and Z. Wu, 'Monolithic integration of InGaAs-GaAs quantum-dot laser and quantum-well electroabsorption modulator on silicon', *IEEE Photon. Technol. Lett.*, vol. 19, pp. 747-749, 2007.
- [3] S. Anantathanasarn, R. Nötzel, P. J. Veldhoven, F. W. M. Otten, Y. Barbarin, G. Servanton, T. Vries, E. Smalbrugge, E. J. Geluk, T. J. Eijkemans, E. A. J. M. Bente, Y. S. Oei, M. K. Smit and J. H. Wolter, 'Lasing of wavelength-tunable (1.55  $\mu\text{m}$  region) InAs/InGaAsP/InP (100) quantum dots grown by metal organic vapor-phase epitaxy', *Appl. Phys. Lett.* vol. 89, pp. 073115, 2006.
- [4] L.W. Shi, Y.H. Chen, B. Xu, Z.C. Wang and Z.G. Wang, 'Effect of inter-level relaxation and cavity length on double-state lasing performance of quantum dot lasers', *Physica E: Low-dimensional Systems and Nanostructures*, vol. 39, pp 203-208, 2007.
- [5] Y. Barbarin, E.A.J.M. Bente, T. de Vries, J.H. den Besten, P.J. van Veldhoven, M.J.H. Sander-Jochem, E. Smalbrugge, F.W.M. van Otten, E.J. Geluk, M.J.R. Heck, X.J.M. Leijtens, J.G.M. van der Tol, F. Karouta, Y.S. Oei, R. Nötzel and M.K. Smit, 'Butt-joint interfaces in InP/InGaAsP waveguides with very low reflectivity and low loss', in *Proc. IEEE/LEOS Symp. Benelux Chapter 2005*, pp. 89-92.
- [6] S. Anantathanasarn, R. Nötzel, P. J. Veldhoven, F. W. M. Otten, T.J. Eijkemans and J.H. Wolter, 'Stacking and polarization control of wavelength-tunable (1.55- $\mu\text{m}$  region) InAs/InGaAsP/InP (100) quantum dots', *Appl. Phys. Lett.* vol. 88, pp. 063105, 2006.
- [7] Y. Barbarin, E.A.J.M. Bente, C. Marquet, E.J.S. Leclère, J.J.M. Binsma and M.K. Smit., 'Measurement of Reflectivity of Butt-Joint Active-Passive Interfaces in Integrated Extended Cavity Lasers', *IEEE Photon. Technol. Lett.*, vol 17, pp. 2265-2267, 2005.